

Electronic and magnetic properties of the new iron-based superconductor $[\text{Li}_{1-x}\text{Fe}_x\text{OH}]\text{FeSe}$

*I. A. Nekrasov⁺¹⁾, M. V. Sadovskii^{+*1)}*

⁺*Institute for Electrophysics UB of the RAS, 620016 Ekaterinburg, Russia*

^{*}*Institute for Metal Physics UB of the RAS, 620290 Ekaterinburg, Russia*

Submitted 26 November 2014

We present the results of paramagnetic LDA band structure calculations: band dispersions, densities of states and Fermi surfaces, for the new iron based high-temperature superconductor LiOHFeSe . Main structural motif providing bands in the vicinity of the Fermi level is FeSe layer which is isostructural to the bulk FeSe prototype superconductor. The bands crossing the Fermi level and Fermi surfaces of the new compound are typical for other iron based superconductors. Experimentally it was shown that introduction of Fe ions into LiOH layer gives rise to ferromagnetic ordering of the Fe ions at $T_C = 10$ K. To study magnetic properties of $[\text{Li}_{0.8}\text{Fe}_{0.2}\text{OH}]\text{FeSe}$ system we have performed LSDA calculations for $\sqrt{5} \times \sqrt{5}$ superlattice and found ferromagnetism within the $\text{Li}_4\text{Fe}(\text{OH})$ layer. To estimate the Curie temperature we obtained Fe – Fe exchange interaction parameters for Heisenberg model from our LSDA calculations, leading to theoretical value of Curie temperature 10.4 K in close agreement with experiment.

DOI: 10.7868/S0370274X15010105

1. Introduction. Novel iron based high-temperature superconductors [1] have been stimulating lots of experimental and theoretical studies since 2008 (extended reviews can be found in [2–6]). There are two large groups of iron-based superconductors: pnictides [2, 3] and chalcogenides [5]. Electronic band structures of these superconductors, as well as some related systems, were compared in Refs. [7, 8].

Among recently synthesized systems particularly interesting is $[\text{Li}_{1-x}\text{Fe}_x\text{OH}](\text{Fe}_{1-y}\text{Li}_y)\text{Se}$ ($x \approx 0.2$, $y \approx 0.08$) compound with [9] the temperature of superconducting transition $T_c = 43$ K and ferromagnetic ordering at Curie temperature $T_C = 10$ K [10].

In this paper we present LDA calculated electronic structure, densities of states and Fermi surfaces for LiOHFeSe system in paramagnetic phase. To investigate ferromagnetism of Fe ions introduced into LiOH layer we performed LSDA calculations for the $[\text{Li}_{0.8}\text{Fe}_{0.2}\text{OH}]\text{FeSe}$ compound. Corresponding values of Heisenberg model exchange parameters obtained from LSDA results were used to calculate Curie temperature, producing a nice agreement with experiments.

2. Electronic structure. The crystal structure of $[\text{Li}_{1-x}\text{Fe}_x\text{OH}](\text{Fe}_{1-y}\text{Li}_y)\text{Se}$ belongs to the primitive tetragonal $P4/nmm$ space group (see table S1 in supplementary materials of Ref. [10]). The LiOHFeSe system has quasi two-dimensional crystal structure of alternat-

ing LiOH and FeSe layers. In Fig. 1 we present an ide-

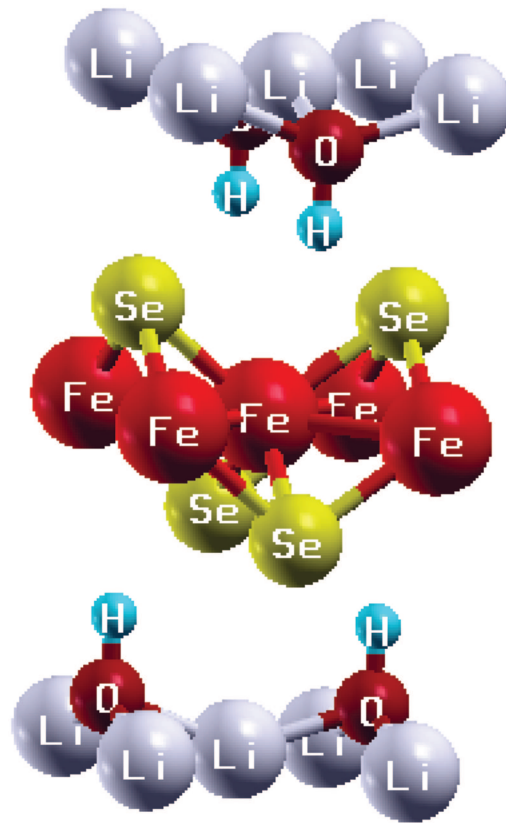


Fig. 1. Crystal structure of LiOHFeSe

¹⁾e-mail: nekrasov@iep.uran.ru; sadovskii@iep.uran.ru

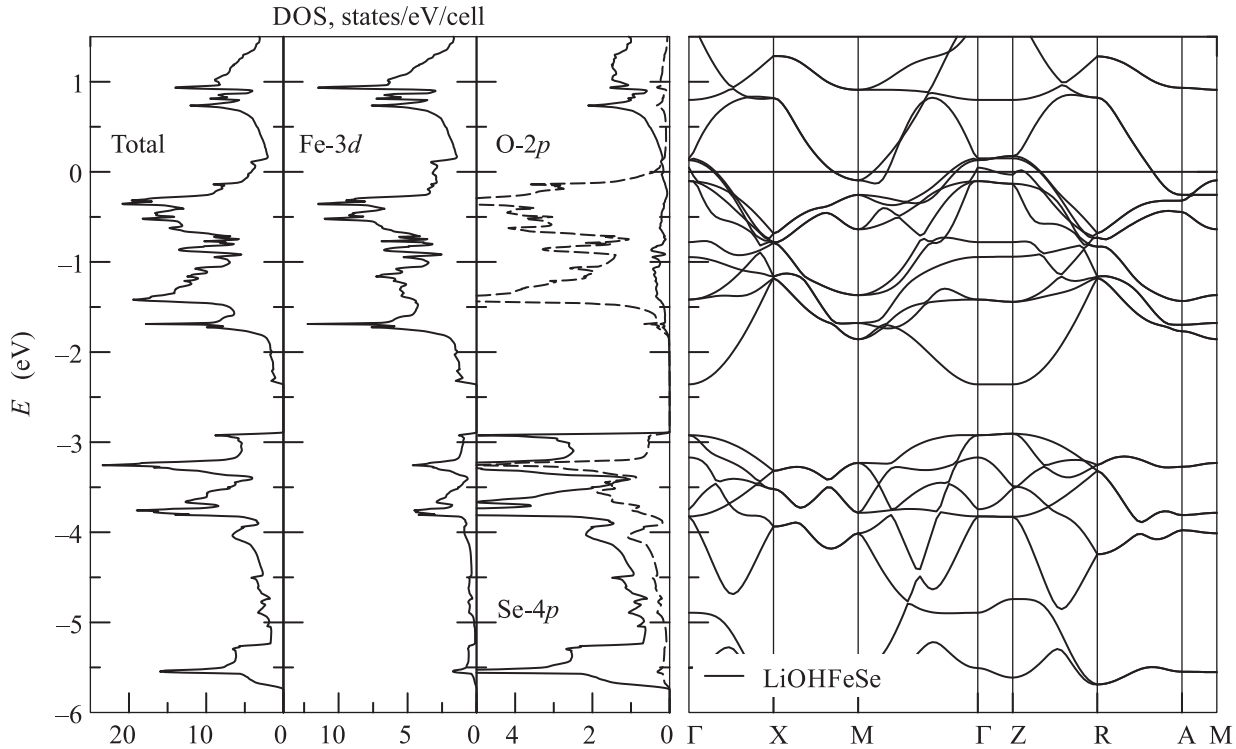


Fig. 2. LDA calculated band dispersions (right) and densities of states (left) of paramagnetic LiOHFeSe. The Fermi level E_F is at zero energy

alised crystal structure of $[Li_{1-x}Fe_xOH](Fe_{1-y}Li_y)Se$. Here we neglect the presence of Li ions in FeSe as well as the presence of Fe ions in the LiOH layers. Also we took Li ion in the $2a$ Wyckoff position instead of $4f$ one. LiOH layer is formed by square lattice of Li ions with OH forming tetrahedra around them. FeSe layer consists of square lattice of Fe ions which are surrounded by tetrahedrally coordinated by Se ions. Actually, this FeSe layer is isostructural to bulk FeSe material [5].

For these idealised crystal structure we have performed LDA band structure calculations within the linearized muffin-tin orbitals method (LMTO) [11] using default settings.

In Fig. 2 we show the calculated LDA band dispersions (on the right) and densities of states (DOS) (on the left). Electronic bands crossing the Fermi level are mostly formed by Fe- $3d$ orbitals and have bandshapes similar to previously studied $BaFe_2As_2$ and FeSe systems (see Refs. [7, 12, 13]). Surprisingly O- $2p$ states are quite close to the Fermi level, beginning just below the Fermi level and going down in energy up to -2 eV. However, there is almost no hybridization between O- $2p$ and Fe- $3d$ states. The Se- $4p$ orbitals form bands at energies below -3 eV. Hybridization between Fe- $3d$ and these Se- $4p$ states is also rather small.

The value of LDA calculated total density of states of LiOHFeSe system at the Fermi level is $N(E_F) = 4.14$ states/cell/eV. Performing simple BCS-like estimates of superconducting critical temperature along the lines of Ref. [7] we obtain $T_c = 36$ K, which is somewhat lower than the experimental value of $T_c = 43$ K [10].

In Fig. 3 LDA present the LDA calculated Fermi surfaces (FS) of LiOHFeSe. In general a shape of the FS of

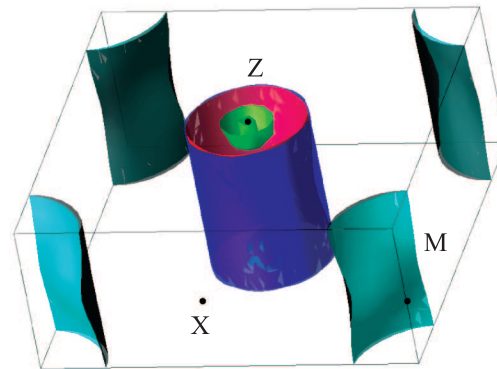


Fig. 3. LDA calculated Fermi surfaces of LiOHFeSe within the first Brillouin zone

LiOHFeSe is typical to iron pnictides or chalcogenides [7, 12, 13]. It has well established cylinders around Γ -

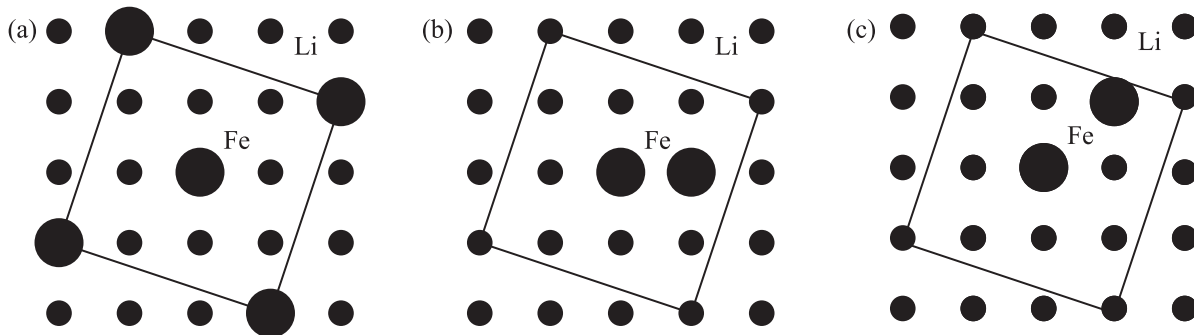


Fig. 4. Possible distributions of Fe ions in Li_4Fe layer. Large circles mark Fe ions, small – Li. Solid line shows $\sqrt{5} \times \sqrt{5}$ unit cell

and M-points. Around Γ point there are two large almost degenerate ideal hole cylinders. Electron cylinders around M-point are slightly corrugated. Also near the Γ -point there is a tiny hole pocket. Some rather small FS sheet appears also around the Z-point.

3. Magnetic structure. As reported in Ref. [10] the introduction of Fe ions into LiOH layer leads to the appearance of ferromagnetism within the layer with Curie temperature about 10 K. To mimic the experimental chemical composition with doping level x about 0.2 we performed LSDA calculations for $\sqrt{5} \times \sqrt{5}$ superlattice, analyzing the several possible magnetic structures, corresponding to different distributions of Fe ions in Li_4Fe layer displayed in Fig. 4. With five formula units for $\sqrt{5} \times \sqrt{5}$ superlattice there can be two ions of Fe in the unit cell with three possible distributions of Fe ions with respect to each other. Corresponding Fe ions are marked as large circles in Fig. 4. Explicit LSDA calculations were made for the most symmetric case shown on the panel (a) of Fig. 4. The other two distributions of Fe ions produce the smaller values of Curie temperature, as was shown for similar situation in Ref. [14].

This LSDA calculation for $(\text{Li}_4\text{Fe})(\text{OH})_5(\text{FeSe})_5$ gives the ferromagnetic solution in agreement with LSDA calculation presented in Ref. [10], with the value of magnetic moment on iron within Li_4Fe layer $\mu_{\text{Fe}} = 3.51 \mu_{\text{B}}$. Corresponding densities of states for 3d states of Fe ion within $\text{Li}_4\text{Fe}(\text{OH})_5$ layer (solid line) and Fe-3d states in FeSe layer (dashed line) are plotted in Fig. 5. We can see that 3d states of Fe ion within $\text{Li}_4\text{Fe}(\text{OH})_5$ layer produce rather narrow spikes in the density of states, which correspond to small amount of Fe ions in the layer. However, the introduction of Fe ions into LiOH layer increases the value of $N(E_{\text{F}})$ up to 4.55 states/cell/eV, and in accordance with the estimates of Ref. [7], this leads to the increase of T_c up to 45 K. Thus, the introduction of additional Fe ions into LiOH layers is important to obtain better agreement with experimental value of $T_c = 43$ K [10].

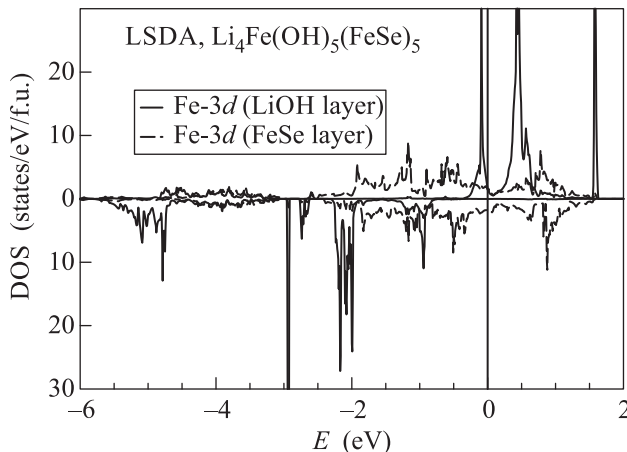


Fig. 5. LSDA calculated densities of states of $(\text{Li}_4\text{Fe})(\text{OH})_5(\text{FeSe})_5$. Solid line corresponds to 3d states of Fe ion within $\text{Li}_4\text{Fe}(\text{OH})_5$ layer, dashed one – Fe-3d states in the FeSe layer. The Fermi level E_{F} is at zero energy

To estimate the Curie temperature we have calculated the values of exchange parameters for the classical Heisenberg model at $T = 0$, using the method proposed in Ref. [15]. The value of nearest neighbor exchange integral obtained for Fe configuration, shown in on Fig. 4a is $J = 1.3$ K. Employing this calculated value of exchange parameter J along with the spin value $S = 2$ (corresponding to experimental observation of Fe^{2+} Mössbauer line in Ref. [10]) we obtain the Curie temperature $T_c = Jz \frac{S(S+1)}{3} = 10.4$ K (where $z = 4$ is the number of nearest neighbors), which is quite close to experimental value of $T_c = 10$ K [10].

4. Conclusion. In this paper we have studied the paramagnetic band structure of the new iron-based high-temperature superconductor $[\text{Li}_{1-x}\text{Fe}_x\text{OH}](\text{Fe}_{1-y}\text{Li}_y)\text{Se}$ (LiOHFeSe) with $T_c = 43$ K [10] by means of LDA band structure calculations, presenting the band dispersions, densities of states and Fermi surfaces. These LDA calculated bands in the

vicinity of the Fermi level as well as Fermi surfaces are typical to other iron – based superconductors. This is obviously due to fact, that the FeSe layers of LiOHFeSe are isostructural to those in the bulk FeSe.

Doping the LiOH layer with Fe ions leads to ferromagnetic ordering of these ions in the layer. Our LSDA calculations confirmed the formation of ferromagnetic structure in LiOH layers and calculated value of exchange interaction has produced the theoretical value of Curie temperature $T_C = 10.4$ K, which agrees rather well with the experimental value of 10 K [10].

We thank M.V. Medvedev for useful discussions. This work is partly supported by RFBR grant # 14-02-00065.

1. Y. Kamihara, T. Watanabe, M. Hirano, and H. Hosono, *J. Am. Chem. Soc.* **130**, 3296 (2008).
2. M. V. Sadovskii, *Uspekhi Fiz. Nauk* **178**, 1243 (2008) [*Physics Uspekhi* **51**(12) (2008)].
3. K. Ishida, Y. Nakai, and H. Hosono, *J. Phys. Soc. Jpn.* **78**, 062001 (2009).
4. D. C. Johnson, *Adv. Phys.* **59**, 803 (2010).
5. Y. Mizuguchi and Y. Takano, *J. Phys. Soc. Jpn.* **79**, 102001 (2010).
6. P. J. Hirshfeld, M. M. Korshunov, and I. I. Mazin, *Rep. Prog. Phys.* **74**, 124508 (2011).
7. M. V. Sadovskii, E. Z. Kuchinskii, and I. A. Nekrasov, *JMMM* **324**, 3481 (2012).
8. I. A. Nekrasov and M. V. Sadovskii, *Pis'ma v ZhETF* **99**, 687 (2014) [*JETP Lett.* **99**(10) (2014)].
9. X. F. Lu, N. Z. Wang, G. H. Zhang, X. G. Luo, Z. M. Ma, B. Lei, F. Q. Huang, and X. H. Chen, *Phys. Rev. B* **89**, 020507(R); X. F. Lu, N. Z. Wang, H. Wu, Y. P. Wu, D. Zhao, X. Z. Zeng, X. G. Luo, T. Wu, W. Bao, G. H. Zhang, F. Q. Huang, Q. Z. Huang, and X. H. Chen, *Nature Materials* (2014); arXiv:1408.2006.
10. U. Pachmayr, F. Nitsche, H. Luetkens, S. Kamusella, F. Brückner, R. Sarkar, H.-H. Klauss, and D. Johrendt, *Angew. Chem. Int. Ed.* **53** (2014).
11. O. K. Andersen, *Phys. Rev. B* **12**, 3060 (1975); O. Gunnarsson, O. Jepsen, and O. K. Andersen, *Phys. Rev. B* **27**, 7144 (1983); O. K. Andersen and O. Jepsen, *Phys. Rev. Lett.* **53**, 2571 (1984).
12. I. A. Nekrasov, Z. V. Pchelkina, and M. V. Sadovskii, *Pis'ma v ZhETF* **88**, 155 (2008) [*JETP Lett.* **88**, 144 (2008)].
13. A. Subedi, L. Zhang, D. J. Singh, and M. H. Du, *Phys. Rev. B* **78**, 134514 (2008).
14. M. V. Medvedev and I. A. Nekrasov, arXiv:1008.3219.
15. A. I. Liechtenstein, M. I. Katsnelson, V. P. Antropov, and V. A. Gubanov, *J. Magn. Magn. Mat.* **67**, 65 (1987); V. I. Anisimov, F. Aryasetiawan, and A. I. Liechtenstein, *J. Phys.: Cond. Matt.* **9**, 767 (1997).